

Linear viscoelastic rheological FrBD models

Luigi Romano^{a,b}, Ole Morten Aamo^b, Jan Åslund^a, Erik Frisk^a

Abstract— In [1], a new modeling paradigm for developing rate-and-state-dependent, control-oriented friction models was introduced. The framework, termed *Friction with Bristle Dynamics* (FrBD), combines nonlinear analytical expressions for the friction coefficient with constitutive equations for bristle-like elements. Within the FrBD framework, this letter introduces two novel formulations based on the two most general linear viscoelastic models for solids: the Generalized Maxwell (GM) and Generalized Kelvin-Voigt (GKV) elements. Both are analyzed in terms of boundedness and passivity, revealing that these properties are satisfied for any physically meaningful parametrization. An application of passivity for control design is also illustrated, considering an example from robotics. The findings of this letter systematically integrate rate-and-state dynamic friction models with linear viscoelasticity.

Index Terms— Friction, friction modeling, rheological models, passivity, passivity-exploiting control

I. INTRODUCTION

Friction plays a central role in the dynamics and control of mechanical systems, particularly in high-precision applications such as robotics, actuators, and mechatronic devices [2]–[5]. Its complex behavior – characterized by pre-sliding displacement, hysteresis, velocity weakening and strengthening effects, and memory – has motivated the development of increasingly sophisticated dynamic friction models. Amongst these, rate-and-state-dependent descriptions, formulated in terms of nonlinear *ordinary differential equations* (ODEs), have proven essential for capturing experimentally observed phenomena that cannot be reproduced by static or purely velocity-dependent laws [6]–[10].

A prominent example is LuGre [6], [7], originally introduced in the context of control-oriented modeling to account for pre-sliding displacement and frictional lag through an internal bristle state. Since its introduction, the LuGre model and its variants have been widely adopted and extended in both theoretical and applied studies, particularly in control design and compensation schemes [2]–[5], [11]. Despite its success, the LuGre model exhibits well-known limitations, most notably the lack of passivity for general parameter choices and operating conditions, unless additional velocity-dependent damping terms are introduced [12]–[14]. This has prompted ongoing research into alternative formulations that preserve physical consistency whilst remaining amenable to analysis and control synthesis [8]–[10].

^a Department of Electrical Engineering, Linköping University, Linköping, Sweden; luigi.romano@liu.se, jan.aslund@liu.se, erik.frisk@liu.se

^b Department of Engineering Cybernetics, NTNU, Trondheim, Norway; ole.morten.aamo@ntnu.no

Recently, a new modeling paradigm termed *Friction with Bristle Dynamics* (FrBD) was introduced in [1] to systematically construct rate-and-state-dependent friction models by combining nonlinear friction laws with constitutive equations describing the internal bristle dynamics. This framework provides a unified and physically grounded approach that naturally incorporates rheological concepts from elasticity and viscoelasticity, allowing friction models to be interpreted as mechanical elements composed of springs and dashpots. Importantly, the FrBD framework enables the derivation of friction models that are inherently bounded and passive under physically meaningful parameterizations [1], properties that are essential for stability and robustness in feedback control systems [15], [16].

Within this context, the present letter extends the FrBD framework by introducing and analyzing a class of nonlinear viscoelastic models inspired by classical linear rheological elements. In particular, formulations based on the Generalized Maxwell (GM) and Generalized Kelvin-Voigt (GKV) representations are developed, allowing for richer descriptions of friction dynamics in solids. The mathematical properties of the resulting model are rigorously investigated, with particular emphasis on existence and uniqueness of solutions, boundedness, and passivity. Beyond theoretical analysis, the letter also examines the qualitative dynamical behavior of the proposed models, showing that they reproduce key friction phenomena such as pre-sliding displacement and frictional hysteresis observed in experimental studies. Finally, the practical relevance of the approach is demonstrated through a control application involving a robotic manipulator, where passivity of the friction model is sapiently exploited for output-feedback control design. This letter develops a unified framework combining general linear viscoelastic theory with rate-and-state-dependent friction laws, resulting in a family of dynamic models that admit clear physical interpretation and systematic characterization using standard engineering methods [22].

Notation and preliminaries

In this letter, \mathbb{R} denotes the set of real numbers; $\mathbb{R}_{>0}$ and $\mathbb{R}_{\geq 0}$ indicate the set of positive real numbers excluding and including zero, respectively. The set of positive integer numbers is indicated with \mathbb{N} , whereas \mathbb{N}_0 denotes the extended set of positive integers including zero, i.e., $\mathbb{N}_0 = \mathbb{N} \cup \{0\}$. $L^p((0, T); \mathbb{R}^n)$ and $C^k([0, T]; \mathbb{R}^n)$ ($p, k \in \{1, 2, \dots, \infty\}$) denotes the spaces of L^p -integrable functions and k -times continuously differentiable functions on $[0, T]$ with values in \mathbb{R}^n (for $T = \infty$, the closure of $[0, T]$ is identified with $\mathbb{R}_{\geq 0}$). For a function $f : (0, T) \mapsto \mathbb{R}$, the sup norm is defined

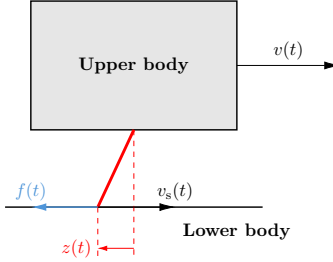


Fig. 1. A schematic representation of the friction model

as $\|f(\cdot)\|_\infty \triangleq \text{ess sup}_{(0,T)} |f(\cdot)|$; $f : (0, T) \mapsto \mathbb{R}$ belongs to the space $L^\infty((0, T); \mathbb{R})$ if $\|f(\cdot)\|_\infty < \infty$. A function $f \in C^0(\mathbb{R}_{\geq 0}; \mathbb{R}_{\geq 0})$ belongs to the space \mathcal{K} if it is strictly increasing and $f(0) = 0$; $f \in \mathcal{K}$ belongs to the space \mathcal{K}_∞ if it is unbounded. A function $f \in C^0(\mathbb{R}_{\geq 0}^2; \mathbb{R}_{\geq 0})$ belongs to the space \mathcal{KL} if $f(\cdot, t) \in \mathcal{K}$ and is strictly decreasing in its second argument, with $\lim_{t \rightarrow \infty} f(\cdot, t) = 0$.

Finally, an application of Theorem 1.1 below will guide the derivation of the rate-and-state-dependent friction models developed in the letter.

Theorem 1.1 (Edwards [17]): Suppose that the mapping $H : \mathbb{R}^{m+n} \mapsto \mathbb{R}^n$ is C^1 in a neighbourhood of a point (x^*, y^*) , where $H(x^*, y^*) = 0$. If the Jacobian matrix $\nabla_y H(x^*, y^*)^T$ is nonsingular, there exist a neighbourhood \mathcal{X} of x^* in \mathbb{R}^m , a neighbourhood \mathcal{Y} of (x^*, y^*) in \mathbb{R}^{m+n} , and a mapping $h \in C^1(\mathcal{X}; \mathbb{R}^n)$ such that $y = h(x)$ solves the equation $H(y, x) = 0$ in \mathcal{Y} . In particular, the implicitly defined mapping $h(\cdot)$ is the limit of the sequence $\{h_k\}_{k \in \mathbb{N}_0}$ of the successive approximations inductively defined by

$$h_{k+1}(x) = h_k(x) - \nabla_y H(x^*, y^*)^{-T} H(x, h_k(x)), \quad (1a)$$

$$h_0(x) = y^*, \quad (1b)$$

for $x \in \mathcal{X}$.

II. MODEL DERIVATION

The present section recapitulates the FrBD framework introduced in [1], which is here generalized to include more complete rheological descriptions of viscoelastic solids. To illustrate the salient aspects of the proposed approach, the situation illustrated schematically in Figure 1 is considered: a rigid body travels with relative velocity $v \in \mathbb{R}$ with respect to a rigid substrate. To the lower boundary of the upper body, deformable bristles are attached, whose deflection is denoted by $z \in \mathbb{R}$. The total sliding velocity between the tip of the bristle and the lower body reads

$$v_s(\dot{z}, v) = v - \dot{z}, \quad (2)$$

where Newton's notation has been adopted for the time derivative, i.e., $\dot{z} = \frac{dz}{dt}$. By deflecting, the bristle generates a force per unit of vertical load, $f \in \mathbb{R}$, which opposes the sliding motion. The dynamic relationship between the bristle deflection and the produced force must be appropriately specified by assuming a constitutive equation. Within the framework of linear viscoelasticity, the GM and GKV elements illustrated in

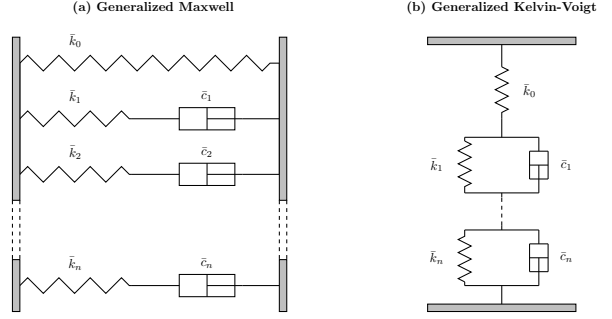


Fig. 2. Linear viscoelastic rheological models for solid elements: (a) Generalized Maxwell (GM); (b) Generalized Kelvin-Voigt (GKV).

Figure 2 provide the most complete rheological descriptions of solids. In particular, adopting a GM model with $n+1$ branches yields

$$f = \bar{k}_0 z + \sum_{i=1}^n f_i, \quad (3a)$$

$$\dot{f}_i = -\tau_i^{-1} f_i + \bar{k}_i \dot{z}, \quad (3b)$$

where $f_i \in \mathbb{R}$, $i \in \{1, \dots, n\}$, denote the internal forces generated by the dissipative branches, $\bar{k}_i \in \mathbb{R}_{>0}$, $i \in \{0, \dots, n\}$, are normalized micro-stiffness coefficients, and $\tau_i \in \mathbb{R}_{>0}$, $i \in \{1, \dots, n\}$, are relaxation time constants. On the other hand, using a GKV provides

$$f = \bar{k}_0 z - \bar{k}_0 \sum_{i=1}^n z_i, \quad (4a)$$

$$f = \bar{k}_i z_i + \bar{c}_i \dot{z}_i, \quad (4b)$$

where $z_i \in \mathbb{R}$, $i \in \{1, \dots, n\}$, represent the internal deformations of the dissipative branches, and $\bar{c}_i \in \mathbb{R}_{>0}$ are normalized micro-damping coefficients.

Equations (3) and (4) are equivalent after a suitable reparametrization, and admit a general representation in the form of the differential constitutive relationship [21]

$$f + \sum_{i=1}^n \gamma_i \frac{d^i f}{dt^i} = \sum_{i=0}^n \sigma_i \frac{d^i z}{dt^i}, \quad (5)$$

where the coefficients γ_i and σ_i can be determined from the original physical parameters. For what follows, (5) is reinterpreted algebraically as

$$f \left(\frac{d^n z}{dt^n}, \dots, \frac{dz}{dt}, z, \frac{d^n f}{dt^n}, \dots, \frac{df}{dt} \right) = \sum_{i=0}^n \sigma_i \frac{d^i z}{dt^i} - \sum_{i=1}^n \gamma_i \frac{d^i f}{dt^i}. \quad (6)$$

In the absence of inertial effects, the force f in (6) must counteract the nondimensional friction force exerted on the tip of the bristle:

$$f_r(v_s(\dot{z}, v)) = \frac{v_s(\dot{z}, v)}{|v_s(\dot{z}, v)|_\varepsilon} \mu(v_s(\dot{z}, v)), \quad (7)$$

where $\mu : \mathbb{R} \mapsto [\mu_{\min}, \infty)$, with $\mu_{\min} \in \mathbb{R}_{>0}$, denotes the friction coefficient, and the function $|\cdot|_\varepsilon \in C^0(\mathbb{R}; \mathbb{R}_{\geq 0})$, with $\varepsilon \in \mathbb{R}_{\geq 0}$, is a regularization of the absolute value $|\cdot|$ for $\varepsilon \in \mathbb{R}_{>0}$, often converging uniformly to $|\cdot|$ in $C^0(\mathbb{R}; \mathbb{R}_{\geq 0})$ for

$\varepsilon \rightarrow 0$ (e.g., $|v|_\varepsilon = \sqrt{v^2 + \varepsilon}$), and with $|\cdot|_\varepsilon \in C^1(\mathbb{R}; \mathbb{R}_{\geq 0})$ for $\varepsilon \in \mathbb{R}_{>0}$ [1]. This letter assumes for simplicity $\mu \in C^0(\mathbb{R}; [\mu_{\min}, \infty))$.

Equating (6) with (7) yields

$$\begin{aligned} H\left(\frac{d^n z}{dt^n}, \dots, \frac{d z}{dt}, z, \frac{d^n f}{dt^n}, \dots, \frac{d f}{dt}, v\right) \\ = f\left(\frac{d^n z}{dt^n}, \dots, \frac{d z}{dt}, z, \frac{d^n f}{dt^n}, \dots, \frac{d f}{dt}\right) - f_r(v_s(\dot{z}, v)) = 0, \\ t \in (0, T), \end{aligned} \quad (8)$$

and invoking Theorem 1.1 with $x \triangleq (z, \frac{d^2 z}{dt^2}, \dots, \frac{d^n z}{dt^n}, \frac{d f}{dt}, \dots, \frac{d^n f}{dt^n}, v)$ and $y \triangleq \dot{z} = \frac{d z}{dt}$ gives

$$\begin{aligned} \dot{z}_{k+1} = \dot{z}_k - \frac{\partial H\left(\frac{d^n z}{dt^n}, \dots, \frac{d z}{dt}, z^*, \frac{d^n f}{dt^n}, \dots, \frac{d f}{dt}, v^*\right)^{-1}}{\partial \dot{z}} \\ \times H\left(\frac{d^n z}{dt^n}, \dots, \frac{d z}{dt}, z, \frac{d^n f}{dt^n}, \dots, \frac{d f}{dt}, v\right), \quad k \in \mathbb{N}_0. \end{aligned} \quad (9)$$

In turn, approximating¹ [1], [23]

$$\frac{\partial H\left(\frac{d^n z}{dt^n}, \dots, \frac{d z}{dt}, z, \frac{d^n f}{dt^n}, \dots, \frac{d f}{dt}, v\right)}{\partial \dot{z}} \approx \sigma_1 + \frac{\mu(v_s(\dot{z}, v))}{|v_s(\dot{z}, v)|_\varepsilon}, \quad (10)$$

recalling (6), and truncating (9) at $k = 1$ gives, for an initial guess $z_0 = 0$,

$$\dot{z}(t) = -\frac{|v(t)|_\varepsilon}{\mu(v(t))} f(t) + v(t), \quad t \in (0, T). \quad (11)$$

Within the linear viscoelastic framework, (11) describes the evolution of the bristle dynamics independently of the assumed constitutive relationship. However, to completely characterize (11), it is again necessary to adopt a specific representation of the bristle element. Using (3) yields the **FrBD_{n+1}-GM** model

$$\dot{z}(t) = -\frac{|v(t)|_\varepsilon}{\mu(v(t))} \left(\bar{k}_0 z(t) + \sum_{i=1}^n f_i(t) \right) + v(t) \quad (12a)$$

$$\dot{f}_i(t) = -\tau_i^{-1} f_i(t) + \bar{k}_i \dot{z}(t), \quad t \in (0, T), \quad i \in \{1, \dots, n\}, \quad (12b)$$

$$z(0) = z_0, \quad f_i(0) = f_{i,0}, \quad i \in \{1, \dots, n\}, \quad (12c)$$

whereas employing (4) delivers the alternative **FrBD_{n+1}-GKV** formulation

$$\dot{z}(t) = -\frac{|v(t)|_\varepsilon}{\mu(v(t))} \bar{k}_0 \left(z(t) - \sum_{i=1}^n z_i(t) \right) + v(t) \quad (13a)$$

$$\begin{aligned} \dot{z}_i(t) = -\frac{\bar{k}_i}{\bar{c}_i} z_i(t) + \frac{\bar{k}_0}{\bar{c}_i} \left(z(t) - \sum_{i=1}^n z_i(t) \right), \\ t \in (0, T), \quad i \in \{1, \dots, n\}, \end{aligned} \quad (13b)$$

$$z(0) = z_0, \quad z_i(0) = z_{i,0}, \quad i \in \{1, \dots, n\}, \quad (13c)$$

¹The approximation is needed to deal with the non-differentiability of the friction force at zero. Informally, for a regularized model, it may be justified by observing that the derivative of $f_r(v)$ at zero will be very large, and can be replaced by $\lim_{v \rightarrow 0} \mu(v)/|v|_\varepsilon = \mu(0)/\varepsilon$.

where the subscript $n+1$ stands for the dynamical order of the system (which coincides with the number of branches in the GM and GKV elements). Equations (12) and (13) generalize the Dahl, LuGre, and FrBD₁-KV model introduced in [1].

III. MODEL PROPERTIES

In this section, the FrBD_{n+1} models (12) and (13) are analyzed in terms of well-posedness, boundedness, and passivity.

A. Well-posedness and steady-state solution

Theorem 3.1 asserts the well-posedness of (12) and (13) under standard assumptions. In the following, the state vector is defined as $\mathbb{R}^{n+1} \ni x(t) \triangleq [z(t) \ f_1(t) \ f_2(t) \ \dots \ f_n(t)]^T$ and $\mathbb{R}^{n+1} \ni x(t) \triangleq [z(t) \ z_1(t) \ z_2(t) \ \dots \ z_n(t)]^T$ for the FrBD_{n+1}-GM and FrBD_{n+1}-GKV variants, respectively.

Theorem 3.1 (Existence and uniqueness of solutions): For all inputs $v \in C^0([0, T]; \mathbb{R})$ and ICs $x(0) = x_0 \in \mathbb{R}^{n+1}$, the FrBD_{n+1} models (12) and (13) admit a unique solution $x \in C^1([0, T]; \mathbb{R}^{n+1})$.

The results of Theorem 3.1 are of a qualitative nature. Formally, the transient solution to (12) and (13) may be recovered using the corresponding state-transition matrix after restating them in state-space representation. However, for large n , closed-form results are not obtainable. Instead, it is interesting to investigate the steady-state solution of (12) and (13). Concerning the force, both variants yield

$$f = \text{sgn}_\varepsilon(v) \mu(v), \quad (14)$$

with $\text{sgn}_\varepsilon(v) \triangleq \frac{v}{|v|_\varepsilon}$. The expressions for the bristle deformation and internal states instead differ for the FrBD_{n+1}-GM and FrBD_{n+1}-GKV models. Starting with (12),

$$z = \frac{f}{\bar{k}_0}, \quad f_i = 0, \quad i \in \{1, \dots, n\}, \quad (15)$$

which coincides with the solution of the LuGre and FrBD₁-KV model introduced in [1], for which $\sigma_0 = \bar{k}_0$. On the other hand, from (13), the following relationships are deduced:

$$z = \sum_{i=0}^n \frac{f}{\bar{k}_i}, \quad z_i = \frac{f}{\bar{k}_i}, \quad i \in \{1, \dots, n\}, \quad (16)$$

which are consistent with the parallel structure of the GKV. In essence, (14)-(16) demonstrate that the FrBD_{n+1} models can reproduce any arbitrary steady-state friction characteristics in solids. The next Section III-B discusses their dynamical features.

B. Mathematical properties

This section investigates the boundedness and passivity properties of the FrBD_{n+1} models (12) and (13). Formal mathematical definitions of these notions are well established in the literature (see, e.g., [18]) and are therefore not repeated here. Instead, their physical interpretation in the context of friction modeling is briefly discussed. In particular, boundedness reflects the physically reasonable expectation that the friction force and internal states remain finite, coherently with (7). On the other hand, passivity captures the intrinsically

dissipative nature of friction, and should be satisfied by any *bona fide* friction model [13]. Essentially, it states that the power exchanged by the friction force must be nonnegative, that is, $pf(t)v(t) \geq 0$, where $p \in \mathbb{R}_{>0}$ is the normal force. For the FrBD_{n+1} models presented in this paper, both boundedness and passivity are always guaranteed.

Starting with the FrBD_{n+1}-GM variant, the following Lyapunov function candidate is considered:

$$V(x(t)) = \frac{1}{2}p\bar{k}_0z^2(t) + \frac{1}{2}\sum_{i=1}^n \frac{p}{\bar{k}_i}f_i^2(t). \quad (17)$$

Differentiating (17) along the dynamics (12), and using (3a), yields

$$\begin{aligned} \dot{V}(t) &= pf(t)v(t) - \frac{p|v(t)|_\varepsilon}{\mu(v(t))}f^2(t) \\ &\quad - \sum_{i=1}^n \frac{p}{\tau_i\bar{k}_i}f_i^2(t), \quad t \in (0, T). \end{aligned} \quad (18)$$

For the FrBD_{n+1}-GKV model, it is convenient to introduce the variable $\mathbb{R} \ni z_0(t) \triangleq z(t) - \sum_{i=1}^n z_i(t)$, whose dynamics obeys

$$\dot{z}(t) = -\frac{|v(t)|_\varepsilon}{\mu(v(t))}\bar{k}_0z_0(t) - \sum_{i=1}^n \dot{z}_i(t) + v(t), \quad t \in (0, T), \quad (19a)$$

$$z_0(0) = z_{0,0}. \quad (19b)$$

Accordingly, the following Lyapunov function candidate is considered:

$$V(x(t)) = \frac{1}{2}p\bar{k}_0z_0^2(t) + \frac{1}{2}\sum_{i=1}^n p\bar{k}_i z_i^2(t). \quad (20)$$

Differentiating (20) along the dynamics (13), and using (4a), gives

$$\begin{aligned} \dot{V}(t) &= pf(t)v(t) - \frac{p|v(t)|_\varepsilon}{\mu(v(t))}f^2(t) \\ &\quad - \sum_{i=1}^n \frac{p}{\bar{c}_i}(\bar{k}_i z_i(t) - \bar{k}_0 z_0(t))^2, \quad t \in (0, T). \end{aligned} \quad (21)$$

The above inequalities (18) and (21) will be instrumental to prove boundedness and passivity for the FrBD_{n+1} models (12) and (13). The main results in this sense are enounced in the following Sections III-B.1 and III-B.2.

1) Boundedness: The next result, formalized in Lemma 3.2, is concerned with the boundedness of the FrBD_{n+1} models.

Lemma 3.2 (Boundedness): Suppose that $|y|_\varepsilon \geq |y|$ for every $y \in \mathbb{R}$. Then, for all inputs $v \in C^0(\mathbb{R}_{\geq 0}; \mathbb{R}) \cap L^\infty(\mathbb{R}_{\geq 0}; \mathbb{R})$ and ICs $x_0 \in \mathbb{R}^{n+1}$, the solutions of (12) and (13) are bounded for all times.

Proof: For brevity, the proof is detailed considering the FrBD_{n+1}-GM formulation; the corresponding result for the FrBD_{n+1}-GKV variant follows from identical arguments.

From (17), it follows the existence of $\gamma_1 \in \mathbb{R}_{>0}$ such that

$$\begin{aligned} \dot{V}(t) &= \gamma_1|v(t)|_\varepsilon \sqrt{V(t)} - \frac{p|v(t)|_\varepsilon}{\mu(v(t))}f^2(t) \\ &\quad - \sum_{i=1}^n \frac{p}{\tau_i\bar{k}_i}f_i^2(t), \quad t \in (0, T). \end{aligned} \quad (22)$$

Moreover, by defining $\mathbb{R}_{>0} \ni \varrho_1 \triangleq \max_{t \in \mathbb{R}_{\geq 0}} |v(t)|_\varepsilon$ and $\mathbb{R}_{>0} \ni \varrho_2 \triangleq \max_{t \in \mathbb{R}_{\geq 0}} \mu(v(t))$, it may be inferred that

$$\begin{aligned} \dot{V}(t) &= \gamma_1|v(t)|_\varepsilon \sqrt{V(t)} \\ &\quad - p|v(t)|_\varepsilon \left(\frac{f^2(t)}{\varrho_2} + \sum_{i=1}^n \frac{p}{\varrho_1\tau_i\bar{k}_i}f_i^2(t) \right) \\ &\leq -|v(t)|_\varepsilon \sqrt{V(t)} \left(\gamma_2 \sqrt{V(t)} - \gamma_1 \right), \quad t \in (0, T). \end{aligned} \quad (23)$$

for some $\gamma_2 \in \mathbb{R}_{>0}$. For all $\sqrt{V(t)} \geq \frac{\gamma_1}{\gamma_2}$, (23) implies $V(t) \leq \max\{V(0), \frac{\gamma_1}{\gamma_2}\}$ for all $t \in [0, T]$, from which the claim follows. \blacksquare

2) Passivity: Passivity is asserted by Lemma 3.3 below.

Lemma 3.3 (Passivity): Consider the FrBD_{n+1} models (12) and (13) with input $v \in C^0([0, T]; \mathbb{R})$ and output $pf \in C^0([0, T]; \mathbb{R})$. Then, the mapping $\Sigma : v \mapsto pf$ is passive with storage functions (17) and (20), respectively.

Proof: Rearranging (18) and (21) and integrating over time immediately yields

$$\int_0^t pf(t')v(t') dt' \geq V(x(t)) - V(x_0), \quad t \in [0, T], \quad (24)$$

with $V(x(t))$ reading respectively as in (17) and (20). \blacksquare

IV. DYNAMICAL BEHAVIOR AND CONTROL APPLICATIONS

The dynamics of the FrBD_{n+1} models is investigated qualitatively in Section IV-A for $n = 1$. Indeed, for $n = 1$, both the GM and GKV variants collapse into a Standard Linear Solid element, for which analytical interconversions are explicitly available in the literature [21]. A control application related to a robotic manipulator is then exemplified in Section IV-B.

A. Dynamical behavior

The dynamical behavior of the FrBD₂ models is discussed concerning *pre-sliding displacement* and *frictional lag*.

1) Pre-sliding displacement: Prior to breakaway, microscopic relative motion occurs as the reactive friction force builds up. This initial regime is commonly referred to as the *pre-sliding displacement*. Courtney-Pratt and Eisner showed that, when the applied external force remains below the breakaway threshold, friction exhibits a behavior analogous to that of a nonlinear spring [19].

To assess whether the FrBD model reproduces this characteristic, a first set of simulations was performed by postulating the friction coefficient as

$$\mu(v_s) = \mu_d + (\mu_s - \mu_d)e^{-(|v_s|/v_s)^\delta}, \quad (25)$$

where $\mu_d, \mu_s \in \mathbb{R}_{>0}$ denote the *dynamic* and *static friction coefficient*, respectively, $v_s \in \mathbb{R}_{\geq 0}$ is the *Stribeck velocity*,

$\delta \in \mathbb{R}_{\geq 0}$ the *Stribeck exponent*. In these simulations, a unit-mass system was subjected to a sinusoidal external force with an amplitude equal to 90% of the breakaway force, whilst varying the excitation frequency over $\omega = 1, 5$, and 10 Hz. The resulting friction force pf is plotted as a function of displacement x in Figure 3(a). The simulated response shows good qualitative agreement with the experimental observations of Courtney-Pratt and Eisner [19], and closely matches the behavior predicted by the LuGre model [7]. Figure 3 was generated using the model parameters listed in Table I, with $\sigma_0 = \bar{k}_1$, $\sigma_1 = \tau_1(\bar{k}_0 + \bar{k}_1)$, and $\gamma_1 = \tau_1$ in (5) according to the GM parametrization.

TABLE I
MODEL PARAMETERS

Parameter	Description	Unit	Value
σ_0	Normalized micro-stiffness	m^{-1}	10^4
σ_1	Normalized micro-damping	s m^{-1}	64.5
γ_1	Relaxation time	s	0.001
μ_d	Dynamic friction coefficient	-	1
μ_s	Static friction coefficient	-	1.5
v_s	Stribeck velocity	m s^{-1}	0.01
δ	Stribeck exponent	-	2
ε	Regularization parameter	$\text{m}^2 \text{s}^{-2}$	0

2) *Frictional lag*: Hess and Soom [20] investigated the velocity-dependent dynamic behavior of friction during unidirectional motion. Their experiments demonstrated the presence of hysteresis in the friction force-velocity relationship: for a given velocity magnitude, the friction force is lower during deceleration than during acceleration. In addition, the width of the hysteresis loop was observed to vary with the rate of change of velocity, expanding or contracting as this rate increases.

For relatively high values of the damping coefficient σ_1 , the hysteresis loop is generally inverted when the Stribeck velocity v_s is sufficiently large. However, the conventional hysteretic behavior is recovered for sufficiently small values of v_s . Figure 3(b) shows the hysteresis curves obtained by imposing relative velocities at different excitation frequencies, $\omega = 25, 50$, and 100 Hz. As the frequency increases, the peak friction force pf decreases, whilst the hysteresis loops become progressively broader, consistent with the preceding discussion.

B. Feedback control of a robotic arm

Inspired by [11], the following example elucidates an application of Lemma 3.3 for output-feedback control design. To this end, the following ODE system, describing a 1-DOF robot manipulator with $\text{FrBD}_{n+1}\text{-GM}$ friction at the joint, is considered [11]:

$$m(q(t))\ddot{q}(t) = -c(q(t), \dot{q}(t))\dot{q}(t) - g(q(t)) - F(t) + U(t), \quad (26a)$$

$$\dot{z}(t) = -\frac{|\dot{q}(t)|_{\varepsilon}}{\mu(\dot{q}(t))} \left(\bar{k}_0 z(t) + \sum_{i=1}^n f_i(t) \right) + \dot{q}(t), \quad (26b)$$

²The results of this section may be easily extended to the case of multi-DOF systems.

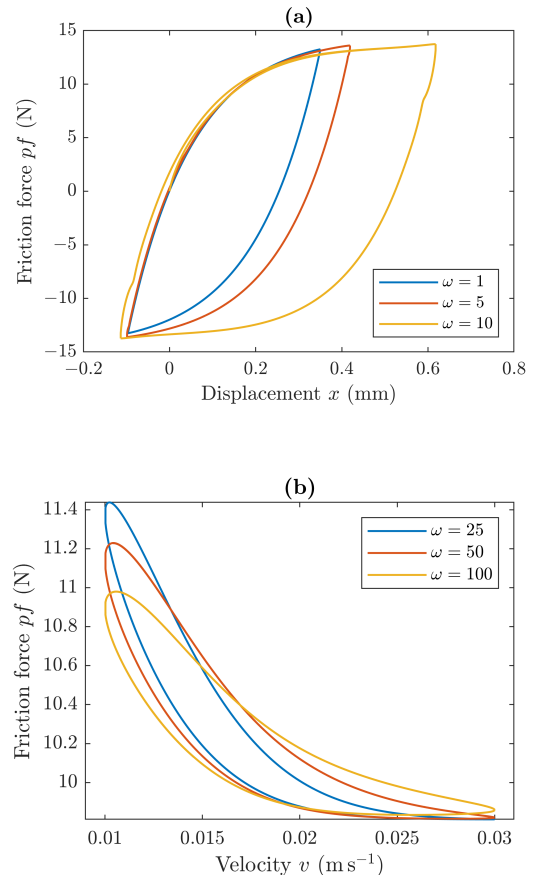


Fig. 3. Dynamical behavior of the FrBD_2 models: (a) Pre-sliding displacement hysteresis; (b) frictional lag hysteresis

$$\dot{f}_i(t) = -\tau_i^{-1} f_i(t) + \bar{k}_i \dot{z}(t), \quad t \in (0, T), \quad i \in \{1, \dots, n\}, \quad (26c)$$

$$q(0) = q_0, \quad \dot{q}(0) = \dot{q}_0, \quad (26d)$$

$$z(0) = z_0, \quad f_i(0) = f_{i,0}, \quad i \in \{1, \dots, n\},$$

where $q(t) \in \mathbb{R}$ denotes the position of the robotic arm, $U(t) \in \mathbb{R}$ the control input, and $\mathbb{R} \ni F(t) \triangleq rpf(t)$ is the friction torque, being $r \in \mathbb{R}_{>0}$ a reference joint radius. In (26a), $m(q(t)) \in \mathbb{R}_{>0}$ is the mass term, $c(q(t), \dot{q}(t))\dot{q}(t) \in \mathbb{R}$ accounts for the Coriolis and centripetal effects, and $g(q(t)) \in \mathbb{R}$ is the gravitational torque. Assuming that $q(t)$ and $\dot{q}(t)$ are measured, the objective consists of tracking a reference position $q_{\text{ref}} \in C^2(\mathbb{R}_{\geq 0}; \mathbb{R})$. Defining $\mathbb{R} \ni \tilde{q}(t) \triangleq q(t) - q_{\text{ref}}(t)$ and $\mathbb{R} \ni s(t) \triangleq \dot{q}(t) + \lambda \tilde{q}(t)$, the control input is specified as [11]

$$U(t) = -k_1 s(t) + \hat{F}(t) + m(q(t))[\ddot{q}_{\text{ref}}(t) - \lambda \dot{\tilde{q}}(t)] + c(q(t), \dot{q}(t))[\dot{q}_{\text{ref}}(t) - \lambda \tilde{q}(t)] + g(q(t)), \quad (27)$$

where $\lambda, k_1 \in \mathbb{R}_{>0}$ are control gains to be selected, and $\mathbb{R} \ni \hat{F}(t) \triangleq rpf(t)$ is an estimate of $F(t)$ obtained using the observer

$$\dot{\tilde{z}}(t) = -\frac{|\dot{q}(t)|_{\varepsilon}}{\mu(\dot{q}(t))} \left(\bar{k}_0 \tilde{z}(t) + \sum_{i=1}^n \hat{f}_i(t) \right) + \dot{q}(t) - k_2 s(t), \quad (28a)$$

$$\dot{\hat{f}}_i(t) = -\tau_i^{-1} \hat{f}_i(t) + \bar{k}_i \dot{\hat{z}}(t), \quad t \in (0, T), \quad i \in \{1, \dots, n\}, \quad (28b)$$

$$\hat{z}(0) = \hat{z}_0, \quad \hat{f}_i(0) = \hat{f}_{i,0}, \quad i \in \{1, \dots, n\}, \quad (28c)$$

where $k_2 \in \mathbb{R}_{>0}$ denotes the observer gain.

Consequently, introducing the error variables $\mathbb{R} \ni \tilde{z} \triangleq z - \hat{z}(t)$, $\mathbb{R} \ni \tilde{f}(t) \triangleq f(t) - \hat{f}(t)$, and $\mathbb{R} \ni \tilde{F}(t) \triangleq F(t) - \hat{F}(t) = rpf(t)$, and using (27), the following system is obtained:

$$m(q(t))\dot{s}(t) = -c(q(t), \dot{q}(t))s(t) - k_1 s(t) - \tilde{F}(t), \quad (29a)$$

$$\dot{\tilde{z}}(t) = -\frac{|\dot{q}(t)|_\varepsilon}{\mu(\dot{q}(t))} \left(\bar{k}_0 \tilde{z}(t) + \sum_{i=1}^n \tilde{f}_i(t) \right) + k_2 s(t), \quad (29b)$$

$$\dot{\tilde{f}}_i(t) = -\tau_i^{-1} \tilde{f}_i(t) + \bar{k}_i \dot{\tilde{z}}(t), \quad t \in (0, T), \quad i \in \{1, \dots, n\}, \quad (29c)$$

$$s(0) = s_0, \quad \tilde{z}(0) = \tilde{z}_0, \quad \tilde{f}_i(0) = \tilde{f}_{i,0}, \quad i \in \{1, \dots, n\}. \quad (29d)$$

From Proposition 2 in [11], it follows that the operator $\Sigma_1 : -\tilde{F} \mapsto s$ defined by (29a) is output-strictly-passive, that is, there exists $\beta_1 \in \mathbb{R}_{>0}$ such that

$$-\int_0^t \tilde{F}(t')s(t') dt' \geq \beta_1 \int_0^t |s(t')|^2 dt', \quad t \in \mathbb{R}_{\geq 0}. \quad (30)$$

Moreover, by Lemma 3.3, the operator $\Sigma_2 : s \mapsto \tilde{F}$ defined by (29b), (29c), and $\tilde{F} = rpf$ is passive. In particular, there exists $\beta_2 \in \mathbb{R}_{\geq 0}$ such that

$$\int_0^t \tilde{F}(t')s(t') dt' \geq -\beta_2. \quad (31)$$

Combining (30) and (31) implies $s \in L^2(\mathbb{R}_{>0}; \mathbb{R})$. Invoking similar arguments as in [11], it may be finally concluded that $\lim_{t \rightarrow \infty} \tilde{q}(t) = 0$. The result is formalized in Theorem 4.1 below.

Theorem 4.1: Consider the ODE system (26) with the observer (28). Then, the control input (27) ensures that $\lim_{t \rightarrow \infty} \tilde{q}(t) = 0$.

An analogous result can be obtained by replacing the FrBD_{n+1}-GM friction model (12) in (26) with the its FrBD_{n+1}-GKV counterpart described by (13).

V. CONCLUSION

This letter presented a class of linear viscoelastic friction models within the Friction with Bristle Dynamics (FrBD) framework, based on the two most general rheological descriptions of solids: the Generalized Maxwell (GM) and Generalized Kelvin-Voigt (GKV) elements.

Utilizing a natural energy-based Lyapunov interpretation, the proposed models, formulated as systems of $n+1$ nonlinear ODEs, were shown to be well-posed and to satisfy boundedness and passivity for all parametrizations. Qualitative analysis demonstrated that key friction phenomena, including pre-sliding displacement and frictional hysteresis, are accurately reproduced and consistent with experimental observations and established dynamic friction models. Finally, a robotic control example illustrated how the passivity of the FrBD model can be effectively exploited in output-feedback control design.

These findings confirm the FrBD framework as a physically grounded and control-oriented approach to dynamic friction

modeling. In particular, the results of this letter unify, for the first time, linear viscoelasticity and rate-and-state friction models. Future extensions may incorporate nonlinear rheological representations.

REFERENCES

- [1] L. Romano, O. M. Aamo, J. Åslund, E. Frisk, "First-order friction models with bristle dynamics: lumped and distributed formulations", under review at IEEE Trans. Contr. Syst. Tech., 2026.
- [2] L. L. B. Yao, Q. Wang and Z. Chen, "Adaptive robust control of linear motors with dynamic friction compensation using modified LuGre model," Automatica, vol. 45, no. 12, pp. 2890-2896, 2009.
- [3] J. Yao, W. Deng and Z. Jiao, "Adaptive Control of Hydraulic Actuators With LuGre Model-Based Friction Compensation," in IEEE Transactions on Industrial Electronics, vol. 62, no. 10, pp. 6469-6477, 2015.
- [4] H. Zeng and N. Sepehri, "Tracking Control of Hydraulic Actuators Using a LuGre Friction Model Compensation," ASME J. Dyn. Sys., Meas., Control, vol. 130, no. 1, pp. 014502, 2008.
- [5] L. Freidovich, A. Robertsson, A. Shiriaev and R. Johansson, "LuGre-Model-Based Friction Compensation," in IEEE Trans. Contr. Syst. Tech., vol. 18, no. 1, pp. 194-200, 2010.
- [6] C. Canudas de Wit, H. Olsson, K. J. Åström and P. Lischinsky, "A new model for control of systems with friction," in IEEE Trans. Auto. Contr., vol. 40, no. 3, pp. 419-425, 1995.
- [7] H. Olsson, "Control Systems with Friction," Doctoral thesis, Department of Automatic Control, Lund Institute of Technology (LTH), 1996.
- [8] F. Al-Bender, V. Lampaert and J. Swevers, "The generalized Maxwell-slip model: a novel model for friction Simulation and compensation," IEEE Trans. Auto. Contr., vol. 50, no. 11, pp. 1883-1887, 2005.
- [9] J. Swevers, F. Al-Bender, C. G. Ganseman and T. Projogo, "An integrated friction model structure with improved presliding behavior for accurate friction compensation," IEEE Trans. Auto. Contr., vol. 45, no. 4, pp. 675-686, April 2000, doi: 10.1109/9.847103.
- [10] V. Lampaert, J. Swevers and F. Al-Bender, "Modification of the Leuven integrated friction model structure," IEEE Trans. Auto. Contr., vol. 47, no. 4, pp. 683-687, 2002, doi: 10.1109/9.995050.
- [11] C. Canudas de Wit, R. Kelly, "Passivity Analysis of a motion control for robot manipulators with dynamic friction", Asian Journal of Control, vol. 9, pp. 30-36, 2007.
- [12] K. J. Åström and C. Canudas-de-Wit, "Revisiting the LuGre friction model," in IEEE Control Systems Magazine, vol. 28, no. 6, pp. 101-114, 2008.
- [13] R. Barabanov and N. Ortega, "Necessary and sufficient conditions for passivity of the LuGre friction model," IEEE Trans. Automat. Contr., vol. 45, no. 4, pp. 830-832, 2000.
- [14] M. F. M. Naser and F. Ikhouane, "Hysteresis loop of the LuGre model," Automatica, vol. 59, pp. 48-53, 2015.
- [15] L. Wu, W. X. Zheng and H. Gao, "Dissipativity-Based Sliding Mode Control of Switched Stochastic Systems," in IEEE Trans. Auto. Contr., vol. 58, no. 3, pp. 785-791, 2013.
- [16] R. Ortega, A. van der Schaft, F. Castanos and A. Astolfi, "Control by Interconnection and Standard Passivity-Based Control of Port-Hamiltonian Systems," IEEE Trans. Auto. Contr., vol. 53, no. 11, pp. 2527-2542, 2008.
- [17] C. H. Edwards, "Advanced Calculus of Several Variables, III - Successive Approximations and Implicit Functions," Academic Press, 1973.
- [18] H. K. Khalil, "Nonlinear Systems," 3rd Edition, Prentice Hall, Upper Saddle River, 2002.
- [19] J. Courtney-Pratt and E. Eisner, "The Effect of a Tangential Force on the Contact of Metallic Bodies," In Proceedings of the Royal Society, vol. A238, pp. 529-550, 1957.
- [20] D. P. Hess and A. Soom, "Friction at a Lubricated Line Contact Operating at Oscillating Sliding Velocities," Journal of Tribology, 112, pp. 147-152, 1990.
- [21] R. J. Loy, F. R. de Hoog, R. S. Anderssen, "Interconversion of Prony series for relaxation and creep," J. Rheol., vol. 59, pp. 1261-1270, 2015.
- [22] A. Sakhnevych, R. Maglione, R. Suero, et al, "Nonlinear mathematical modeling of frequency-temperature dependent viscoelastic materials for tire applications," Nonlinear Dyn, vol. 112, pp. 21729-21750, 2024.
- [23] G. Rill, T. Schaeffer and M. Schuderer, "LuGre or not LuGre," Multi-body Syst Dyn, vol. 60, pp. 191-218, 2024, doi: 10.1007/s11044-023-09909-5.